buildings

Article

Mechanical Property and Dimensional Stability of Chopped Basalt Fiber-Reinforced Recycled Concrete and Modeling with Fuzzy Inference System

Chu-Jie Jiao [1,2], Xiu-Cheng Zhang [1,2], Wei-Zhi Chen [3] and Xue-Fei Chen [1,2,3,4,*]

1 Engineering Research Center of Disaster Prevention and Mitigation of Southeast Coastal Engineering Structures (JDGC03), Fujian Province University, Putian 351100, China
2 Institute of Civil Engineering, Putian University, Putian 351100, China
3 School of Civil Engineering, Guangzhou University, Guangzhou 510006, China
4 Joint Key Laboratory of the Ministry of Education, Institute of Applied Physics and Materials Engineering, University of Macau, Avenida da Universidade, Taipa, Macau SAR 999078, China
* Correspondence: chenxuefei@gzhu.edu.cn

Abstract: The rising amount of construction and demolition wastes (C & DWs) is triggering serious environmental and social problems globally. This study conducted an experimental investigation of basalt fiber (BF)-reinforced concrete with recycled aggregates (RAs) sourced from C & DWs. The flexural strength, the flexural to compressive strength ratio, and the drying shrinkage are set as indicators for the evaluation of the coupling effect of BF and RA in concrete. Results show that BF generated a significant effect on the flexural strength until the BF dosage was no higher than 1%. The excessive mixing amount of BF, though it still contributed to a positive effect on elevating the flexural strength, was of a reduced utility. Regarding the flexural to compressive strength ratio (denoted as ratio), BF and RA jointly produced a positive synergistic effect. In addition, the BF was verified as competent in curbing the adverse effect of RA incorporation upon the drying shrinkage. Relative to the benchmark concrete which contains 100% RA and no BF, 1% BF contributed to a 31.6% reduction in the drying shrinkage. The results prove that BF reinforcement is a feasible and promising approach to curb the drawbacks of RA concrete.

Keywords: construction wastes; recycled aggregates; recycled concrete

Citation: Jiao, C.-J.; Zhang, X.-C.; Chen, W.-Z.; Chen, X.-F. Mechanical Property and Dimensional Stability of Chopped Basalt Fiber-Reinforced Recycled Concrete and Modeling with Fuzzy Inference System. *Buildings* **2023**, *13*, 97. https://doi.org/10.3390/buildings13010097

Academic Editors: Long Li, Shipeng Zhang, Xiaosheng Li and Jie Xiao

Received: 25 November 2022
Revised: 24 December 2022
Accepted: 27 December 2022
Published: 30 December 2022

1. Introduction

Billions of construction and demolition wastes (C & DWs) are generated yearly around the world. The landfilling approach is no longer suitable to treat C & DWs, considering the environmental issues and the rising price of land resources. Instead, a promising method is to crush those wastes into recycled aggregates for the preparation of functional mortar or recycled concrete [1–3]. However, embrittlement limits the practical application of concrete, especially recycled concrete. Fibers, the materials enhancing toughness, are thereby added into recycled concrete, aiming to both facilitate ductility and retard deterioration of the end products. It was found that an appropriate amount of fiber enhanced the impact resistance and lifted splitting tensile strength, as well as bending strength [4,5]. Fiber in concrete also effectively improves the fracture toughness and post-bending cracking behavior of the mixture. Attributing to the bridging effect and the three-dimensional distribution, the existence of fibers decreases the width and number of cracks [6–8] and therefore facilitates the durability of concrete [9,10], including wear resistance and freeze–thaw resistance [11].

Typical fibers frequently used by researchers in their studies are steel fiber, carbon fiber, glass fiber, polypropylene fibers, bio-fibers [9,12–14], and basalt fiber (BF) [8]. The chopped BF is extracted from basalt by the thermochemical process. BF is obtained by melting acid basalt at about 1400 °C. The dominant mineral compositions of basalt are plagioclase, pyroxene, and olivine. The diameter and length of basalt fiber are in general within the range of 10–20 μm and 3–130 mm [15]. A notable advantage of BF is that it consumes less energy during manufacturing and is cheaper than glass or carbon fiber [16]. According to thermogravimetry, the thermal stability of basalt fiber (above 40 °C) is better than that of glass fiber. It was reported that the onset temperature of basalt fiber is c.a. 205 °C; whilst its counterpart, glass fiber, is just ~163 °C [17]. The crystallization behavior and the presence of iron oxide in BF enhance the thermal stability of BF [18,19]. BF also has high tensile strength and elongation before breaking, endowing the composite with high sustainability and impact resistance. Concerning the chemical durability of BF, it is observed that BF has poor acid resistance, but a better alkali resistance [20]. After corrosion treatment, the mechanical properties of BF are better than those of glass fiber. BF is therefore a good substitute for glass fiber to reinforce concrete that has an alkaline environment.

However, previous articles take less consideration of the indicator of the flexural to compressive strength ratio and sparsely address the dimensional stability, which is a key controlling aspect of the quality of concrete, alongside the mechanical property. This paper therefrom conducted an experimental investigation on BF-reinforced RA concrete and probes into both the mechanical strength and the dimensional stability. A mathematical model based on the fuzzy inference system is established to fit and predict the compressive strength of basalt fiber-reinforced recycled concrete with varied content of recycled aggregates on different curing days.

2. Experimental Details

2.1. Materials

Table 1 summarizes the key physical properties of the raw materials. The cement is ordinary Portland cement with a strength grade of 52.5 and an apparent density of 3120 kg/m^3 as per the Chinese standard [21]. The river sand (RS) is medium sand in zone II as per the Chinese standard [22]. Natural aggregate (NA) is crushed granite stone, whilst recycled aggregate (RA) is retrieved from crushed recycled concrete. The obtained RA belongs to grade II RA, as per the Chinese standard [23], and is used in previous papers [24–28]. Both NA and RA are divided into two categories according to the size, viz., 4.75–9.5 mm and 9.5–19 mm. The above two kinds of aggregates are blended into the mixture with a mass ratio of 7:3. A high-performance water reducing agent (Model: Q8081, liquid) is used to control the slump of fresh concrete. The BF is a commercially available product purchased from the market.

Table 1. Physical properties of raw materials.

Raw Materials	Cement	RS	NA	RA	BF
Apparent density (kg/m^3)	3120	2573	2660	2387	2650
Water absorption (%)	-	0.87	0.45	3.75	0.79
Crushing index (%)	-	-	4.7	10.3	-
Fineness modulus	-	2.52	-	-	-
Cut length (mm)	-	-	-	-	8–12
Tensile strength (MPa)	-	-	-	-	4850
Elastic modulus (GPa)	-	-	-	-	87

Note: RS-river sand, NA-natural aggregate, RA-recycled aggregate, BF-basalt fiber.

2.2. Sample Preparation

Table 2 depicts the designed and adjusted mix proportion of the concrete based on the absolute volume method as per a Chinese standard [29]. RAs were used to replace NAs in volumetric dosages of 0, 25, 50, 75, and 100%, whereas BFs were used to reinforce the recycled concrete at five levels of 0, 0.25, 0.5, 0.75, 1, and 1.5 vol.%. Some supplementary water was added to the mixture to ensure the RAs reached the saturated surface dry (SSD) status. A polycarboxylate superplasticizer with the appropriate dosage was used to achieve a target slump equivalent to 160–180 mm. The fresh mixture was poured into steel molds covered with plastic films for 24 h and then de-molded and transferred to a standard curing chamber

(20 ± 2 °C, >95% RH) until the testing. Regarding the drying shrinkage test, samples were at first pre-cured in the standard curing chamber (20 ± 2 °C, 95% RH) for 3 d and then moved to the indoor area with constant temperature and humidity (20 ± 2 °C, 60 ± 5% RH).

Table 2. Mix proportion of the concrete (kg/m^3).

Code	Cement	Water	RS	BF	NA	RA	S.W.	W.R.
RA0BF0.00 (control)	400	180	964.2	0	924.7	-	0	0.32
RA0BF0.25	400	180	957.8	6.3	924.7	-	0	1.21
RA0BF0.50	400	180	951.3	13	924.7	-	0	1.77
RA0BF0.75	400	180	944.9	19.6	924.7	-	0	2.63
RA0BF1.00	400	180	938.5	26.2	924.7	-	0	3.16
RA0BF1.50	400	180	925.6	39.5	924.7	-	0	3.52
RA25BF0.00	400	180	964.2	0	693	205.7	5.4	0.58
RA25BF0.25	400	180	957.8	6.3	693	205.7	5.4	1.47
RA25BF0.50	400	180	951.3	13	693	205.7	5.4	2.03
RA25BF0.75	400	180	944.9	19.6	693	205.7	5.4	2.89
RA25BF1.00	400	180	938.5	26.2	693	205.7	5.4	3.42
RA25BF1.50	400	180	925.6	39.5	693	205.7	5.4	3.78
RA50BF0.00	400	180	964.2	0	461.2	413.6	11.6	0.83
RA50BF0.25	400	180	957.8	6.3	461.2	413.6	11.6	1.72
RA50BF0.50	400	180	951.3	13	461.2	413.6	11.6	2.28
RA50BF0.75	400	180	944.9	19.6	461.2	413.6	11.6	3.14
RA50BF1.00	400	180	938.5	26.2	461.2	413.6	11.6	3.67
RA50BF1.50	400	180	925.6	39.5	461.2	413.6	11.6	4.03
RA75BF0.00	400	180	964.2	0	229.5	621.6	17.8	1.1
RA75BF0.25	400	180	957.8	6.3	229.5	621.6	17.8	1.99
RA75BF0.50	400	180	951.3	13	229.5	621.6	17.8	2.55
RA75BF0.75	400	180	944.9	19.6	229.5	621.6	17.8	3.41
RA75BF1.00	400	180	938.5	26.2	229.5	621.6	17.8	3.94
RA75BF1.50	400	180	925.6	39.5	229.5	621.6	17.8	4.3
RA100BF0.00	400	180	964.2	0	-	829.6	24	1.31
RA100BF0.25	400	180	957.8	6.3	-	829.6	24	2.2
RA100BF0.50	400	180	951.3	13	-	829.6	24	2.76
RA100BF0.75	400	180	944.9	19.6	-	829.6	24	3.62
RA100BF1.00	400	180	938.5	26.2	-	829.6	24	4.15
RA100BF1.50	400	180	925.6	39.5	-	829.6	24	4.51

Note: RS-river sand, BF-basalt fiber, NA-natural aggregate, RA-recycled aggregate, S.W.-supplementary water, W.R.-water reducer.

2.3. Testing

2.3.1. Determination of Mechanical Strength

The compressive strength and flexural strength of hardened samples were tested as per a Chinese standard [30]. A universal pressing machine was used to determine the compressive strength of concrete cubes (100 × 100 × 100 mm) (Equation (1) and Figure 1) and the flexural strength of concrete cuboids (100 × 100 × 400 mm) (see Equation (2) and Figure 2).

$$f_c = \frac{F}{A} \quad (1)$$

$$f_f = \frac{Fl}{bh^2} \quad (2)$$

where

f_c means the compressive strength of cubic concrete specimens (MPa), accurate to 0.1 MPa;
f_f means the flexural strength of concrete specimens (MPa), accurate to 0.01 MPa;
F means the failure load (N);
A means the bearing area (mm^2);
l means the span between supports (mm);
h means the height of the cross-section (mm);
b means the width of the cross-section (mm).

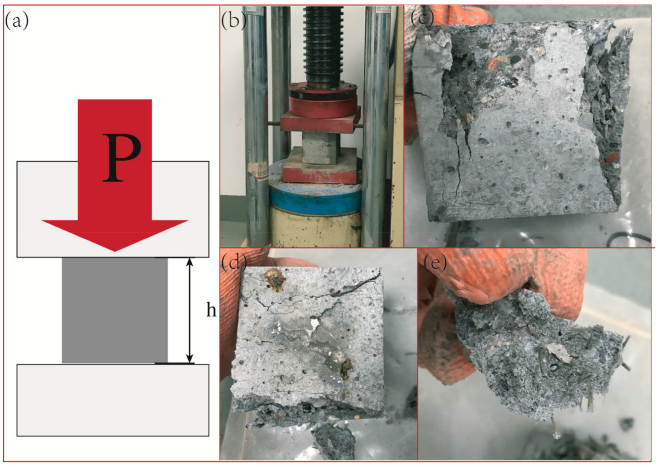

Figure 1. Compressive strength test: (**a**) schematic representation of the compressive strength test; (**b**) in-site compressive strength test; (**c**–**e**) crushed concrete samples.

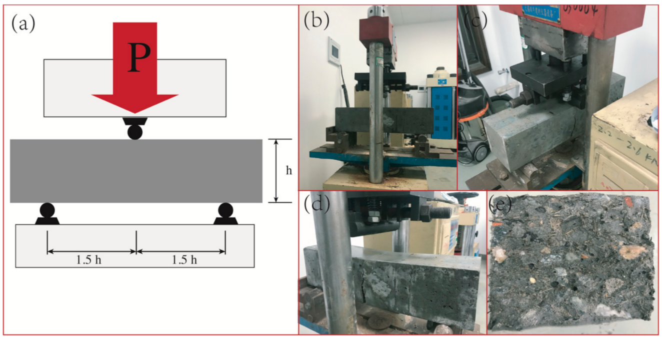

Figure 2. Flexural strength test: (**a**) schematic representation of the flexural strength test; (**b**–**d**) in-site flexural strength test; (**e**) a cross-section of broken concrete samples.

2.3.2. Determination of the Drying Shrinkage

The drying shrinkage of the specimens (100 × 100 × 515 mm cuboids) was calculated as per Equation (3) [31]. The target test time counted from the time when the specimens were transferred to the indoor area.

$$\varepsilon_{st} = \frac{L_0 - L_t}{L_b} \tag{3}$$

where

ε_{st} means the drying shrinkage of concrete at t-d (t starts from the time to measure the initial length);

L_0 means the initial length (mm);

L_b means the gauge length (mm);

L_t means the length at t-d (mm).

2.4. Modeling Conformation

The modeling with a fuzzy inference system is primarily divided into 4 parts: data input, fuzzy inputs by membership functions, fuzzy inference by IF-THEN rules, and de-fuzzy outputs. In this study, the gbell function is used for fuzzy inputs, whilst the linear function and the weighted average are used for de-fuzzy outputs.

3. Results and Discussion

3.1. Flexural Strength

Figure 3 shows the 28 d flexural strength of the concrete, where the increment represents the increase of the latter value relative to the previous one. The impact of RA content on flexural strength is limited. When the content of BF is 1%, using 100% RA to replace NA reduces the flexural strength from 6.48 MPa to 6.08 MPa, with a reduced rate of 6.17%. When the RA content maintains 100%, the flexural strength ascends with the increase in BF content. BF at the dosage of 0.25%, 0.5%, 0.75%, 1%, and 1.5%, respectively, leads the flexural strength to increase by 6.81%, 17.02%, 33.80%, 41.72%, and 43.27%%, relative to RA100BF0. This is because the addition of BF makes the hardened concrete form an effective integration. When the fiber–concrete composite is subjected to the external load, the external load can be relatively evenly distributed on the whole bearing surface. In this way, the generation of cracks on the weak section to a great extent is limited, to avoid the rapid damage to the whole. Secondly, BF has the effect of crack resistance. To some extent, the fibers with three-dimensional random and uniform distribution prevent crack growth. Finally, when the hardened concrete hardens and shrinks, some microcracks appear. The existence of BF reduces the shrinkage of concrete to a certain extent and further reduces the possibility of shrinkage cracks. However, the marginal utility of the fiber decreases gradually. For each 0.25%, values of the relative increment of the flexural strength are respectively 6.8%, 10.2%, 16.8%, 7.9%, and 1.5%. This is because the 1% BF is deemed enough to curb the generation and propagation of cracks in concrete, whilst too many fibers introduce extra void to the concrete due to the agglomeration effect and the extra interactive interfaces between BF and the surrounding matrix.

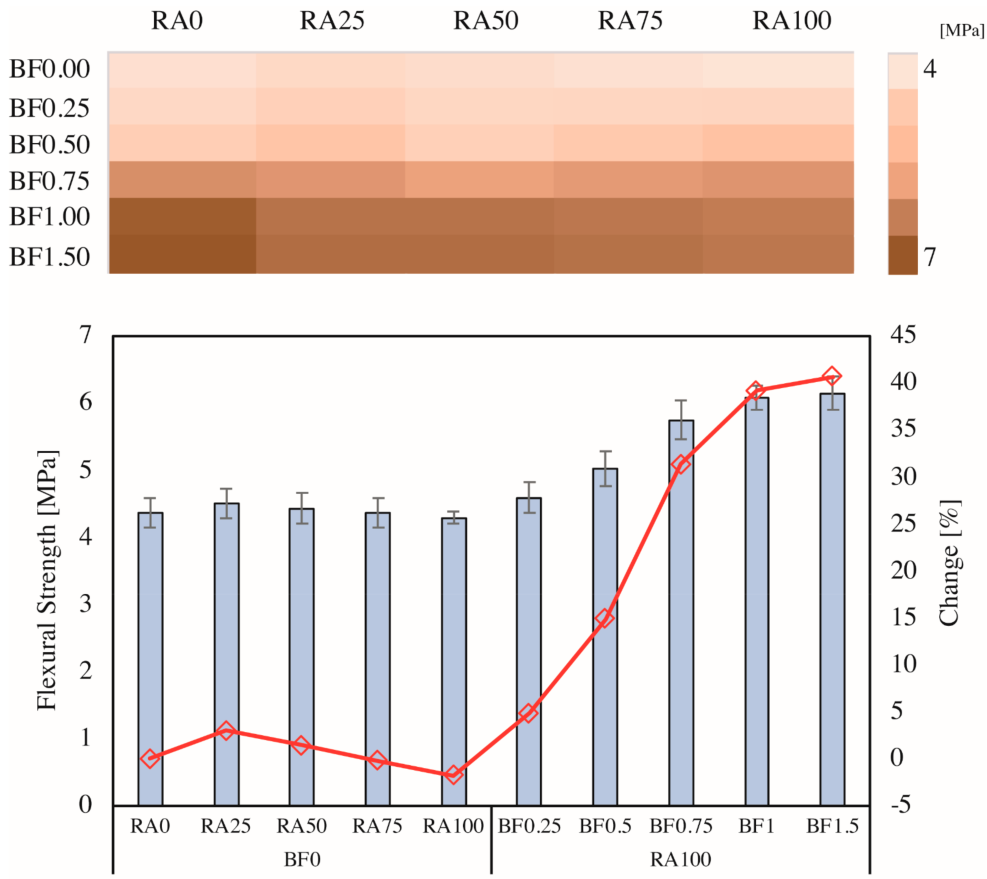

Figure 3. Flexural strength of concrete with various recycled aggregate (RA) and basalt fiber (BF) content, and the relative flexural strength (RA0BF0 as the benchmark).

3.2. Flexural to Compressive Strength Ratio

The flexural to compressive strength ratio (hereafter denoted as the ratio) is the ratio of the flexural strength to the compressive strength of the concrete. The larger the ratio, the better the crack resistance of the concrete. Therefore, it is an important index to measure the performance of fiber-reinforced concrete. Figure 4 shows the 28 d ratio (the ratio of 28 d flexural strength to 28 d compressive strength) of the BF-reinforced RA concrete. As is shown by the color bar of the 3D surface and the contour map, a lighter color means a bigger value. The increase in RA content and BF dosage jointly makes the ratio head towards the upper right corner which holds the brightest color, leading to the conclusion that both the content of BF and the replacement rate of RA have positive effects on the ratio.

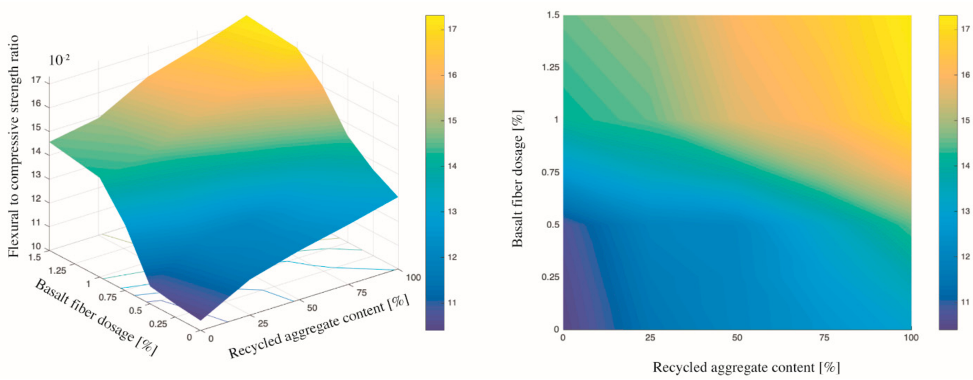

Figure 4. Flexural to compressive strength ratios of concrete with various recycled aggregate (RA) and basalt fiber (BF) content [Note: 3D surface (**left**); contour map (**right**)].

When the replacement rate of RA is 100%, values of the ratio of concrete with 0%, 0.25%, 0.5%, 0.75%, 1%, and 1.5% BF are, respectively, 0.1303, 0.1363, 0.1449, 0.1604, 0.1706, and 0.1732, with the changes (Benchmark: RA100BF0) as 4.63%, 11.23%, 23.13%, 30.97%, and 32.91%. This is because the addition of BF increases both flexural strength and compressive strength, but the relative increase rate of flexural strength is greater than that of compressive strength. The effect of BF on the growth of flexural strength is more significant.

Regarding the relative growth rate (the latter value relative to the former value), when the content of BF increases from 0.5% to 0.75% and from 0.75% to 1%, the relative growth values of the ratio are 11.9% and 7.84%, respectively. However, when the content of BF is further increased from 1% to 1.5%, the relative increase of the ratio is only 1.94%. When the content of BF is less than 1%, the unit fiber content possesses a significant effect on the increase of the ratio, but with a further increase in the fiber content, the improvement effect is gradually weakened. Compared with RA0BF1, 25%, 50%, 75%, and 100% RA replacement increases the ratio by 2.5%, 10%, 14.2%, and 20.4%, respectively, when the fiber content is 1%. This is because RA has a lower hardness relative to NA. It leads to the decrease in compressive strength of RA concrete with the increase in the replacement rate of RA. However, the old mortar on the surface of RA can improve the new interface transition zone to a certain extent, which offsets the defects of low hardness. It reduces the flexural strength of RA concrete, but the reduction is not as significant as that of the compressive strength. The aforementioned content results in a phenomenon that RA relative to NA has a positive effect on enhancing the ratio. In conclusion, both the BF and the RA are positively related to the ratio of RA concrete, viz., they have a positive synergistic effect.

3.3. Drying Shrinkage

In addition to the mechanical properties represented by strength, the dimensional stability represented by deformation is also an important index to measure the quality of concrete. Under the joint action of external load and environment, concrete produces deformation which further triggers microcracks, and cracks significantly impact the mechanical and durable performance of concrete. The hardened concrete, with the combined action of ambient temperature and humidity, bears the thermal shrinkage related to the cooling process and the drying shrinkage related to the water loss. The effect of thermal shrinkage on non-mass concrete is not important. Therefore, this study probes into drying shrinkage and sets it as the embodiment of the dimensional stability.

The internal moisture migrates and dissipates when the hardened concrete is placed in an environment with low humidity. It makes the concrete fail to maintain its dimensional stability so that dry shrinkage happens. Figure 5 shows the dry shrinkage of the BF-reinforced RA concrete at 90 d. Overall, the dry shrinkage of concrete increases with the increase in the replacement rate of RA, and decreases with the increase in the content of BF. Specifically, when the content of BF is controlled to be 1%, the dry shrinkage values of concrete with 0%, 25%, 50%, 75%, and 100% RA are, respectively, 2.439, 2.69, 2.865, 3.024, and 3.244 $\times$ 10^{-4}. The changes relative to RA0BF1 are correspondingly 0, 10.28, 17.45, 23.99, and 33.0%. This is because the increase in RA leads to an increase in mortar (the sum of old mortar and new mortar) in concrete. However, the water absorption of mortar is higher than that of aggregates. When the environmental humidity is unsaturated, a higher mortar proportion results in higher water loss and correspondingly higher drying shrinkage. In addition, RA has a large porosity because of its porous structure and many microcracks on the surface of old mortar. These pores provide holes and channels for water to escape in the process of concrete drying, accelerating the process of water migration and evaporation, and weakening the water retention performance. This also leads to a positive correlation between RA content and drying shrinkage. On the contrary, when the RA dosage is 100%, the drying shrinkage values of concrete with 0, 0.25, 0.5, 0.75, 1, and 1.5% BF are, respectively, 4.743, 3.951, 3.828, 3.415, 3.244, and 3.320 $\times$ 10^{-4}. Compared with RA100BF0, the values of the reduction rate are, respectively, 0, 16.7, 19.3, 28, 31.6, and 30%. The dominating reason for the inhibition effect of BF on the dry shrinkage is that the existence of fiber reduces the generation of microcracks and limits the development of cracks, which can be verified by micrographs in Figure 4. It thus blocks the passage of water escape, enhances the water retention, and weakens the drying shrinkage deformation. In addition, the three-dimensional disordered network structure formed by the BF shapes a supporting structure which also inhibits the drying shrinkage to a certain extent.

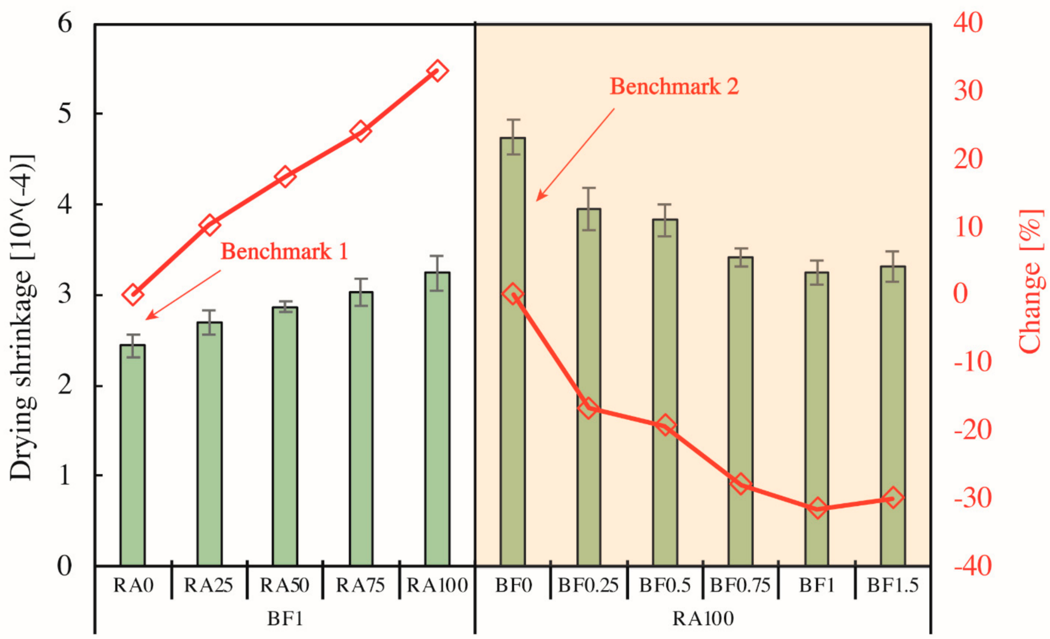

Figure 5. Drying shrinkage of concrete with various recycled aggregate (RA) and basalt fiber (BF) content.

3.4. Mechanism Analysis

Plain recycled concrete is usually a brittle material with low tensile strength and poor cracking resistance. The brittleness of recycled concrete can be improved to some extent by incorporating chopped basalt fibers. Figure 6 illustrates the fracture surface of the chopped basalt fiber-reinforced recycled concrete. As can be seen from the figure, the basalt fibers act as a bridge at the macroscopic level, limiting the development and extension of cracks in the concrete. When fiber-reinforced concrete is subjected to external loads, microcracks are generated inside the concrete. As the cracks gradually extend to the fibers, the interface between the fibers and the concrete is debonded due to tensile stresses perpendicular to the direction of crack development. When the crack develops to the interface, the stress concentration at the end of the crack is reduced, thus reducing the crack generation and preventing the crack development. In addition, when microcracks develop, chopped basalt fibers generate a filling effect, suturing the adjacent surfaces on both sides of the crack and improving the internal structure of the concrete concurrently. When microcracks further extend, the interaction between the basalt fibers and the concrete matrix reduces the width and area of the microcracks. After the concrete cracks, the three-dimensional mesh structure formed by the basalt fibers in the matrix further modifies the cracks and transfers and disperses the surrounding stresses. The incorporation of basalt fibers therefore limits the generation and development of microcracks in recycled concrete, improving the mechanical properties. However, the excessive incorporation of basalt fibers tends to lead to uneven fiber dispersion in the concrete, resulting in voids in the fiber–concrete boundary and negatively affecting the mechanical properties of the concrete. Therefore, when using basalt fibers to reinforce recycled concrete, care should be taken to ensure that the fibers are uniformly dispersed in the concrete matrix so that they are not heavily agglomerated and distributed along the crack direction.

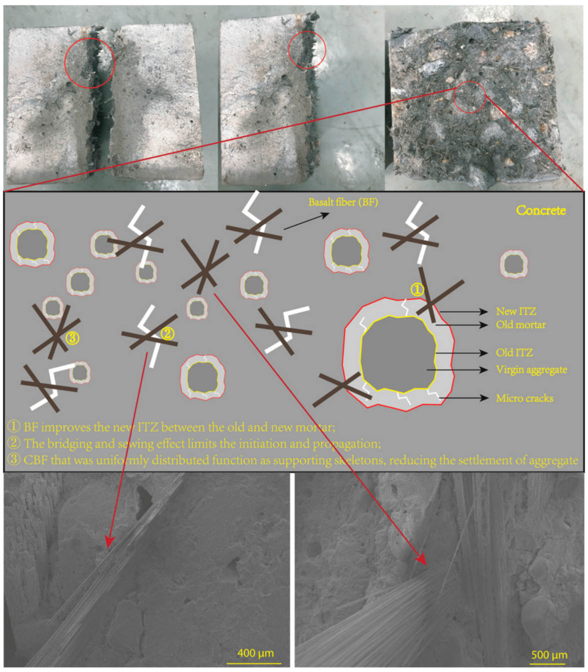

Figure 6. Macro- and micro-graphs of the basalt fiber-reinforced recycled concrete and the diagrammatic sketch: macro-graph (**top**); sketch (**middle**); micro-graph (**bottom**).

3.5. Modeling

Relative to the artificial neural networks that set the computing process as a 'black box', a key advantage of the fuzzy inference model is it is mathematically explainable.

The compressive strength (output) can be calculated based on the following equations, Equations (4) and (5).

$$MF = gbellmf(x, [a_1, a_2, a_3]) = \frac{1}{\left(1 + abs\left(\frac{x-a_3}{a_1}\right)\right)^{2a_2}} \tag{4}$$

where the x indicates inputs and [a,b,c] indicate parameters shown by Table 3.

$$\begin{array}{c} Output = \frac{1}{9} \times ([input1MF1 + input2MF1 + b_1] + [input1MF1 + input2MF2 + b_2] \\ +[input1MF1 + input2MF3 + b_3] + [input1MF2 + input2MF1 + b_4] \\ +[input1MF2 + input2MF2 + b_5] + [input1MF2 + input2MF3 + b_6] \\ +[input1MF3 + input2MF1 + b_7] + [input1MF3 + input2MF2 + b_8] \\ +[input1MF3 + input2MF3 + b_9]\# \end{array} \tag{5}$$

where b_i (i = 1 to 9) is the parameter with values available in Table 4.

Table 3. Values of parameters of membership functions in the fuzzy model.

		a_1	a_2	a_3
Input1	MF1	25.00	2.00	−5.47
	MF2	25.00	2.00	50.00
	MF3	25.00	2.00	100.00
Input2	MF1	45.00	1.98	−0.02
	MF2	45.00	1.98	90.00
	MF3	45.00	1.99	180.00

Table 4. Values of parameters of the output function in the fuzzy model.

b_1	b_2	b_3	b_4	b_5	b_6	b_7	b_8	b_9
20.12	56.40	49.65	17.63	53.93	47.12	15.69	45.12	43.12

The calculation process can be sketched by Figure 7 and visually presented by Figure 8.

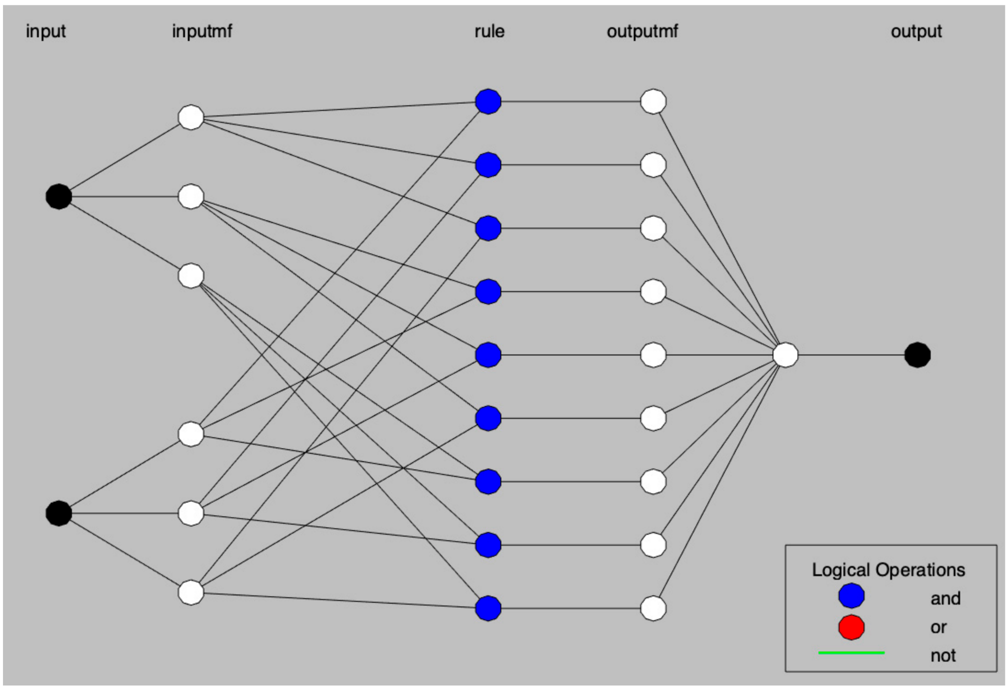

Figure 7. The structure of the fuzzy model.

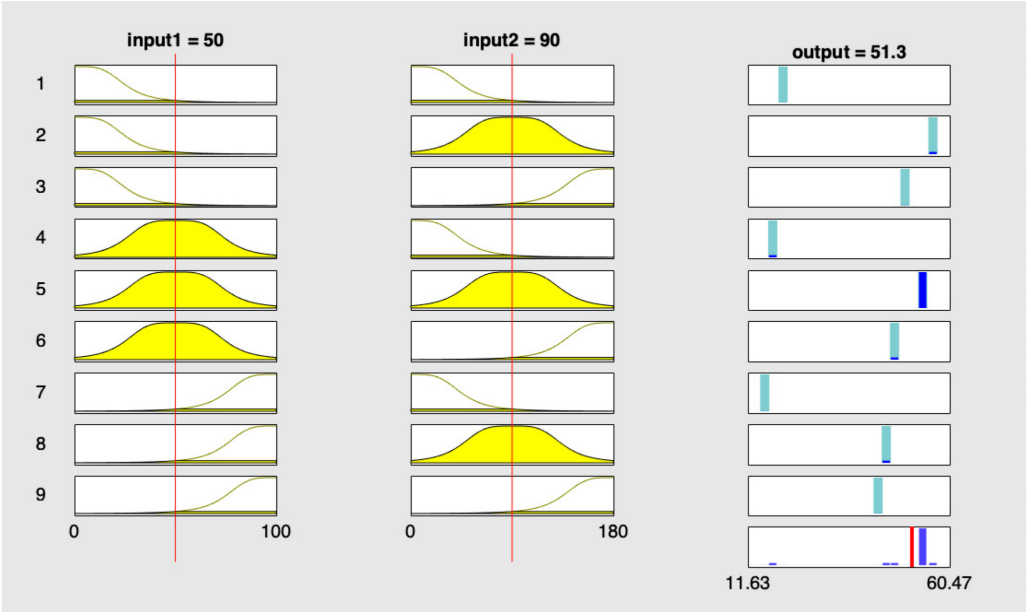

Figure 8. A typical rule view of the fuzzy model [recycled aggregates dosage (input1) = 50%, curing days (input2) = 90 d].

Figure 9 exhibits the respond surface and the contour map of the compressive strength of concrete with varied recycled aggregate dosages at different curing times. It is noted that the content of recycled aggregates negatively affects the compressive strength at all curing ages, whereas as the curing time prolongs, the extent of this negative impact gradually declines. The compressive strength at 180 d is almost dosage independent as per the right subgraph of Figure 7. This phenomenon can be explained as follows. The compressive strength of concrete is overall determined by the hardness of aggregates, the content of binding materials, the water to binder ratio, the interfacial transition zone, etc. Among these factors, the strength of coarse aggregates and the hydration level of cementitious materials are the two leading determinants. Initially, at the early curing age, the first factor plays a more influential role because the hydration just started. As the hydration further develops, cementitious materials gradually generate strength via the growing content of hydration products. The hardness of recycled aggregate is constant, whilst the strength of binding materials is increasing. This indicates a threshold. When this threshold is breached, the strength of binding materials takes the lead and becomes the most dominating influential factor, covering and offsetting the fading impact of aggregates.

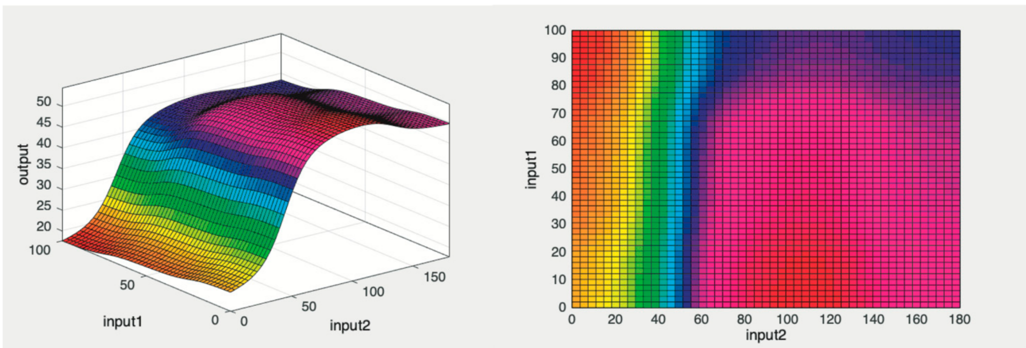

Figure 9. Respond surface (**left**) and contour map (**right**) of fiber-reinforced recycled aggregate concrete (input 1 indicates the content of recycled aggregate, %; input 2 indicates the curing time, d; the height means the compressive strength corresponding to varied input values, MPa).

4. Conclusions

Based on the above, the following conclusions can be drawn:

- BF lifts the flexural strength of RA concrete because of the crack curbing effect and the three-dimensional distribution of fibers in the surrounding mixture. However, the effect is significant only when the BF dosage is no higher than 1 vol.% because the fiber in the excessive content tends to agglomerate.
- Both BF and RA promote the concrete towards a higher flexural to compressive strength ratio. The positive synergistic effect is on one hand caused by the restriction effect of crack propagation and development, and on the other hand attributed to the unbalanced effect generated by the RA upon the compressive strength and the flexural strength.
- BF is proven to effectively curb the drying shrinkage of RA concrete, with the maximized value of reduction reaching c.a. 30%. It strengthens the dimensional stability and promotes the durable performance of RA concrete, facilitating the scale reutilization of C & DWs.

Author Contributions: C.-J.J.: Project administration, funding acquisition, writing—review and editing. X.-C.Z. and W.-Z.C.: Conceptualization, carrying out all the measurements and experiments, methodology, writing—review and editing. X.-F.C.: Project administration, funding acquisition, writing—review and editing. All authors have read and agreed to the published version of the manuscript.

Funding: This research was funded by [the National Natural Science Foundation of China] grant number [No. 52078148 and 52108125], [Special Research Projects in Key Areas for Colleges and Universities in Guangdong Province (Science and Technology Plan for Rural Revitalization)] grant number [No. 2021ZDZX4009], [Natural Science Foundation of Guangdong Province, China] grant number [No. 2022A1515010038], [Key Innovation Program of Water Conservancy Science and Technology of Guangdong Province] grant number [No. 2017-32], [Basic Research Program (Municipality-University joint fund) of Science and Technology Bureau of Guangzhou] grant number [No. SL2023A03J00880], [Scientific Research Project of Education Bureau of Guangzhou] grant number [No. 202235263], [Zhuhai Municipal Science and Technology Planning Project in the Field of Social Development] grant number [No. ZH22036201210032PWC], [Engineering Research Center of Disaster Prevention and Mitigation of Southeast Coastal Engineering Structures of Fujian Province University] grant number [NO. 2022001].

Acknowledgments: Special thanks to the 'Testing Technology Center for Materials and Devices of Tsinghua Shenzhen International Graduate School' for providing testing related service. The first author would also like to thank the 'Minjiang River Scholar Program' for supporting this research.

Conflicts of Interest: The authors declare no conflict of interest.

References

1. Chen, X.-F.; Kou, S.-C.; Poon, C.S. Rheological behaviour, mechanical performance, and NOx removal of photocatalytic mortar with combined clay brick sands-based and recycled glass-based nano-TiO_2 composite photocatalysts. *Constr. Build. Mater.* **2020**, *240*, 117698. [CrossRef]
2. Chen, X.-F.; Jiao, C.-J. Microstructure and physical properties of concrete containing recycled aggregates pre-treated by a nano-silica soaking method. *J. Build. Eng.* **2022**, *51*, 104363. [CrossRef]
3. Chen, X.-F.; Lin, S.-R.; Kou, S.-C. Effect of composite photo-catalysts prepared with recycled clay brick sands and nano-TiO_2 on methyl orange and NOx removal. *Constr. Build. Mater.* **2018**, *171*, 152–160. [CrossRef]
4. Hsie, M.; Tu, C.; Song, P.S. Mechanical properties of polypropylene hybrid fiber-reinforced concrete. *Mater. Sci. Eng. A* **2008**, *494*, 153–157. [CrossRef]
5. Banthia, N.; Chokri, K.; Ohama, Y.; Mindess, S. Fiber-reinforced cement based composites under tensile impact. *Adv. Cem. Based Mater.* **1994**, *1*, 131–141. [CrossRef]
6. Spadea, S.; Farina, I.; Carrafiello, A.; Fraternali, F. Recycled nylon fibers as cement mortar reinforcement. *Constr. Build. Mater.* **2015**, *80*, 200–209. [CrossRef]
7. Izaguirre, A.; Lanas, J.; Alvarez, J.I. Effect of a polypropylene fibre on the behaviour of aerial lime-based mortars. *Constr. Build. Mater.* **2011**, *25*, 992–1000. [CrossRef]
8. Chen, X.-F.; Kou, S.-C.; Xing, F. Mechanical and durable properties of chopped basalt fiber reinforced recycled aggregate concrete and the mathematical modeling. *Constr. Build. Mater.* **2021**, *298*, 123901. [CrossRef]

9. Chen, X.-F.; Quan, C.-Q.; Jiao, C.-J. Experimental Study of Chloride Resistance of Polypropylene Fiber Reinforced Concrete with Fly Ash and Modeling. *Materials* **2021**, *14*, 4417. [CrossRef]
10. Wang, L.; Zeng, X.; Li, Y.; Yang, H.; Tang, S. Influences of MgO and PVA Fiber on the Abrasion and Cracking Resistance, Pore Structure and Fractal Features of Hydraulic Concrete. *Fractal Fract.* **2022**, *6*, 674. [CrossRef]
11. Grdic, Z.J.; Curcic, G.A.T.; Ristic, N.S.; Despotovic, I.M. Abrasion resistance of concrete micro-reinforced with polypropylene fibers. *Constr. Build. Mater.* **2012**, *27*, 305–312. [CrossRef]
12. Wang, L.; He, T.; Zhou, Y.; Tang, S.; Tan, J.; Liu, Z.; Su, J. The influence of fiber type and length on the cracking resistance, durability and pore structure of face slab concrete. *Constr. Build. Mater.* **2021**, *282*, 122706. [CrossRef]
13. Wang, L.E.I.; Guo, F.; Yang, H.; Wang, Y.A.N.; Tang, S. Comparison Of Fly Ash, PVA Fiber, MgO And Shrinkage-Reducing Admixture On The Frost Resistance Of Face Slab Concrete Via Pore Structural And Fractal Analysis. *Fractals* **2021**, *29*, 2140002. [CrossRef]
14. Chen, X.F.; Kou, S.C.; Xing, F. Effect of agriculture and construction wastes on the properties of magnesium oxychloride cement mortar with tourmaline powder. *Materials* **2019**, *12*, 115. [CrossRef] [PubMed]
15. Fiore, V.; Scalici, T.; Di Bella, G.; Valenza, A. A review on basalt fibre and its composites. *Compos. Part B Eng.* **2015**, *74*, 74–94. [CrossRef]
16. Dhand, V.; Mittal, G.; Rhee, K.Y.; Park, S.-J.; Hui, D. A short review on basalt fiber reinforced polymer composites. *Compos. Part B Eng.* **2015**, *73*, 166–180. [CrossRef]
17. Hao, L.C.; Yu, W.D. Evaluation of thermal protective performance of basalt fiber nonwoven fabrics. *J. Therm. Anal. Calorim.* **2010**, *100*, 551–555. [CrossRef]
18. Moiseev, E.A.; Gutnikov, S.I.; Malakho, A.P.; Lazoryak, B.I. Effect of iron oxides on the fabrication and properties of continuous glass fibers. *Inorg. Mater.* **2008**, *44*, 1026–1030. [CrossRef]
19. Gutnikov, S.I.; Malakho, A.P.; Lazoryak, B.I.; Loginov, V.S. Influence of alumina on the properties of continuous basalt fibers. *Russ. J. Inorg. Chem.* **2009**, *54*, 191–196. [CrossRef]
20. Ramachandran, B.E.; Velpari, V.; Balasubramanian, N. Chemical durability studies on basalt fibres. *J. Mater. Sci.* **1981**, *16*, 3393–3397. [CrossRef]
21. *JG/T 315*; Natural Pozzolanic Materials Used for Mortar and Concrete. Standardization Administration of the People's Republic of China: Beijing, China, 2011.
22. *JGJ 52*; Standard for Technical Requirements and Test Method of Sand and Crushed Stone (or Gravel) for Ordinary Concrete. Standardization Administration of the People's Republic of China: Beijing, China, 2006.
23. *GB/T 25177*; Recycled Coarse Aggregate for Concrete. Standardization Administration of the People's Republic of China: Beijing, China, 2010.
24. Chen, X.-F.; Jiao, C.-J. Effect of construction wastes on the rheo-physical behavior of photocatalytic mortar. *Case Stud. Constr. Mater.* **2022**, *16*, e01049. [CrossRef]
25. Chen, X.-F.; Jiao, C.-J. Experimental Investigation and Modeling of the Sulfur Dioxide Abatement of Photocatalytic Mortar Containing Construction Wastes Pre-Treated by Nano TiO_2. *Catalysts* **2022**, *12*, 708. [CrossRef]
26. Chen, X.-F.; Jiao, C.-J. A photocatalytic mortar prepared by tourmaline and TiO_2 treated recycled aggregates and its air-purifying performance. *Case Stud. Constr. Mater.* **2022**, *16*, e01073. [CrossRef]
27. Chen, X.-F.; Jiao, C.-J. Effect of physical properties of construction wastes based composite photocatalysts on the sulfur dioxide degradation: Experimental investigation and mechanism analysis. *Case Stud. Constr. Mater.* **2022**, *17*, e01237. [CrossRef]
28. Chen, X.-F.; Kou, S.-C. Sulfur Dioxide Degradation by Composite Photocatalysts Prepared by Recycled Fine Aggregates and Nanoscale Titanium Dioxide. *Nanomaterials* **2019**, *9*, 1533. [CrossRef] [PubMed]
29. *JGJ 55*; Specification for Mix Proportion Design of Ordinary Concrete. Standardization Administration of the People's Republic of China: Beijing, China, 2011.
30. *GB/T 50081*; Standard for Test Methods of Mechanical Properties on Ordinary Concrete. Standardization Administration of the People's Republic of China: Beijing, China, 2019.
31. *GB/T 50082*; Standard for Test Methods of Long-Term Performance and Durability of Ordinary Concrete. Standardization Administration of the People's Republic of China: Beijing, China, 2009.